inorganics

MDPI

Article

Influence of Nanoscale Surface Arrangements on the Oxygen Transfer Ability of Ceria–Zirconia Mixed Oxide

Eleonora Aneggi *, Carla de Leitenburg and Alessandro Trovarelli

Dipartimento Politecnico di Ingegneria e Architettura, Università di Udine, 33100 Udine, Italy; carla.deleitenburg@uniud.it (C.d.L.), alessandro.trovarelli@uniud.it (A.T.)

* Correspondence: eleonora.aneggi@uniud.it; Tel.: +39-0432-558830

Received: 28 April 2020; Accepted: 11 May 2020; Published: 12 May 2020

Abstract: Ceria-based materials, and particularly CeO_2–ZrO_2 (CZ) solid solutions are key ingredient in catalyst formulations for several applications due to the ability of ceria to easily cycling its oxidation state between Ce^{4+} and Ce^{3+}. Ceria-based catalysts have a great soot oxidation potential and the mechanism deeply relies on the degree of contact between CeO_2 and carbon. In this study, carbon soot has been used as solid reductant to better understand the oxygen transfer ability of ceria–zirconia at low temperatures; the effect of different atmosphere and contact conditions has been investigated. The difference in the contact morphology between carbon soot and CZ particles is shown to strongly affect the oxygen transfer ability of ceria; in particular, increasing the carbon–ceria interfacial area, the reactivity of CZ lattice oxygen is significantly improved. In addition, with a higher degree of contact, the soot oxidation is less affected by the presence of NO_x. The NO oxidation over CZ in the presence of soot has also been analyzed. The existence of a core/shell structure strongly enhances reactivity of interfacial oxygen species while affecting negatively NO oxidation characteristics. These findings are significant in the understanding of the redox chemistry of substituted ceria and help determining the role of active species in soot oxidation reaction as a function of the degree of contact between ceria and carbon.

Keywords: ceria–zirconia; redox activity; soot oxidation; ball milling

1. Introduction

Ceria-based materials, and particularly CeO_2–ZrO_2 (CZ) solid solutions are key ingredient in catalyst formulations for several applications due to the ability of ceria to easily cycling its oxidation state between Ce^{4+} and Ce^{3+} [1–3]. Undoubtedly, its major technological application is the depollution of noxious compounds from internal combustion engines [4,5]. The wide success of ceria-based materials is strictly correlated to its oxygen storage capacity (OSC). Ceria based catalysts are able to modulate the available oxygen releasing it under reducing conditions and taking up oxygen under oxidizing conditions [1,2,5–7]. The removal/uptake of oxygen from the fluorite lattice is of fundamental importance in several catalytic applications. The redox/oxygen storage properties of ceria are at the origin for its widely application in formulations for diesel soot oxidation [8,9] and many studies investigate the role of ceria-based catalyst in carbon soot oxidation [10–20]. Specifically, the production of "active oxygen species" is believed to be among the most important features and several authors focused on the reaction mechanism in order to better elucidate the formation and the role of "active oxygen" [21–26]. We pointed out that two different mechanisms coexist during soot oxidation [21], one related to the amount of surface available oxygen and one associated to the amount of bulk oxygen; their relative significance on the overall reaction is dependent over ceria-soot

interface and to the accessibility of O_2 gas phase. Machida et al. [27] focused on the generation of "active oxygen" in the form of superoxide (O_2^-) ions upon interaction of the O_2 gas phase with surface oxygen vacancies of reduced ceria. The mechanism is associated to the availability of adsorbed active oxygen species (peroxide and superoxide), which spill over onto the soot surface resulting in the formation of vacant sites, which are then filled with gas-phase O_2. The mechanism is strictly affected by the degree of contact between soot and the ceria-based catalyst [28] and the temperature of soot oxidation dramatically decreases when an intimate contact is used. Recently, we observed that the interface between soot and ceria at a nanoscale level could dramatically influence the transfer of active oxygen from ceria to carbon boosting soot oxidation activity [28–30].

In this study carbon soot has been used as reductant to investigate the oxygen transfer of ceria at low temperature and obtain further insight on its oxygen storage properties and on the role of the carbon–ceria interface in oxygen exchange. For this purpose, a sample of ceria–zirconia particles of composition $Ce_{0.8}Zr_{0.2}O_2$ was mixed with carbon soot to obtain different degrees of contact between carbon and catalyst. In addition to loose and tight contact carbon and ceria–zirconia were mixed in a high-energy mill to promote the formation of a core of oxide particles wrapped in a thin carbon envelope, which strongly improves contact (supertight contact) and contributes to lower soot oxidation temperatures [28]. Here, the effect of various oxidation atmospheres (O_2, $NO+O_2$ and NO_2+O_2) has been investigated at different contact conditions. The presence of a core/shell carbon/ceria structure strongly enhances the reactivity of interfacial oxygen species while affecting negatively NO oxidation characteristics. This is due to the carbon envelope, which hinders NO interaction with ceria–zirconia while promoting vacancy formation at the interface with successive generation of active oxygen species. These findings are significant in the understanding of the redox chemistry of ceria and doped ceria based materials.

2. Results and Discussion

2.1. Textural and Structural Characterization

A sample of ceria–zirconia particles of nominal composition $Ce_{0.8}Zr_{0.2}O_2$ was mixed with soot using different approaches in order to obtain a carbon/catalyst composite with varying degrees of contact between the two components. Conventional catalyst/soot mixtures were obtained in tight and loose contact mode by mixing the appropriate amount of ceria–zirconia with soot (Printex U by Degussa) in an agate mortar for 10 min or mixing with a spatula for 2 min, respectively. Improved contact (supertight contact) was achieved in a high-energy Spex mill equipped with zirconia balls and jar. In a typical experiment ceria–zirconia particles were milled with soot for 8 h [28].

Composition, BET surface area and apparent density of materials are reported in Table 1. While mixing soot in the loose and tight mode did not affect surface area, the high energy milling process induced a significant surface area loss (from 79 to 29 m^2/g) that was typically observed upon milling of a high-surface-area powder that is presumably due to adhesion of fine particles on the surfaces of larger agglomerates [5,31]. Similarly, an increase in the apparent density of the powder was observed due to the milling process (from 1.45 to 1.65 g/mL).

Table 1. Characteristics of the materials.

Sample	Name	SA (m^2/g)	Apparent Density (g/mL)	Crystallite Size (nm) [a]	Cell Parameter [b] (nm)	Molar Composition [b]	Free ZrO_2 [c] (%)
$Ce_{0.8}Zr_{0.2}O_2$	CZ	79	1.45	6	5.3590(4)	$Ce_{0.82}Zr_{0.18}O_2$	/
$Ce_{0.8}Zr_{0.2}O_2$/C loose	CZ(l)	79	1.44	6	5.3586(4)	$Ce_{0.82}Zr_{0.18}O_2$	/
$Ce_{0.8}Zr_{0.2}O_2$/C tight	CZ(t)	78	1.45	6	5.3588(4)	$Ce_{0.82}Zr_{0.18}O_2$	/
$Ce_{0.8}Zr_{0.2}O_2$/C milled	CZ(m)	29	1.65	14	5.3487(2)	$Ce_{0.78}Zr_{0.22}O_2$	10

[a] calculated with Scherrer formula from X-ray diffraction patterns. [b] from Rietveld refinement. [c] amount of free ZrO_2 originating from abrasion during milling obtained from Rietveld refinement.

XRD peaks for CZ, CZ(l) and CZ(t) were broad and the values of the crystallite size obtained according to the Scherrer equation [32] was about 6 nm; after milling, peaks became more intense, clear and well defined (Figure 1), with an increase of crystallite size to 14 nm together with a drop in surface area. The milling process induces contamination of the CZ sample with a small amount of free ZrO_2 originating from the milling media, as evidenced by XRD profiles (Figure 1), while no reaction between CZ and carbon was highlighted. Rietveld refinement of XRD profiles revealed also a zirconia enrichment of ceria–zirconia solid solution with a decrease of cell parameter in agreement with the introduction of the smaller Zr^{4+} in the lattice.

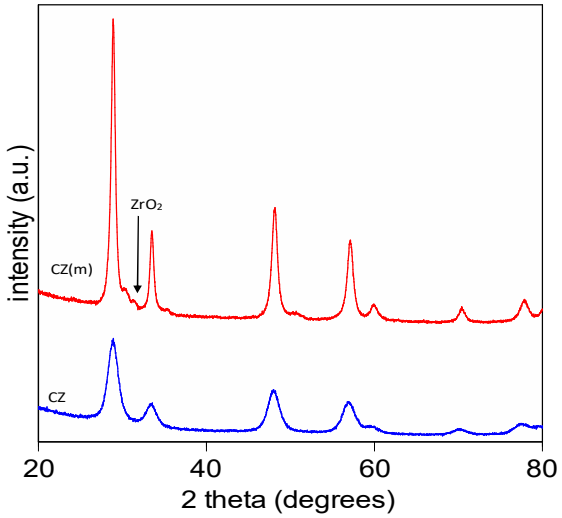

Figure 1. XRD profile for ceria–zirconia before and after high energy milling.

2.2. Catalytic Activity

In the present study the effect of a different atmosphere and contact conditions on soot combustion over the $Ce_{0.8}Zr_{0.2}O_2$ catalyst was studied to better understand the oxygen transfer ability of ceria–zirconia at low temperatures. Soot combustion at different contact conditions in oxidizing (air) and in inert (N_2) atmosphere was investigated by means of thermogravimetry experiments (Figure 2). Under oxidizing conditions, a complete soot combustion was achieved for all samples independent of the degree of contact. However, the type of contact dramatically affected the activity and increasing the soot/catalyst contact, a large decrease in the temperature of 50% soot conversion (T50) was observed with CZ(m) already removing 50% of carbon at temperature lower than 268 °C, compared to 364 °C and 534 °C, for CZ(t) and CZ(l) respectively. This behavior originates from the different morphology of the ceria–zirconia/carbon interface that in the case of the loose and tight contact mode was characterized by the presence of carbon on ceria–zirconia surface in the form of large particle aggregates with a modest degree of contact, while after high energy milling, soot aggregates progressively disappeared and carbon could be observed prevalently as a thin shell over the CZ crystallites [28–30]. This morphology favors the redox mechanism and activates the transfer of the surface/bulk oxygen of ceria–zirconia to carbon, strongly affecting soot oxidation activity. As previously reported, this enhancement is observed only by milling simultaneously ceria–zirconia and carbon soot [28]; the individual and separate milling of ceria–zirconia and carbon did not affect the material and did not change/promote the redox/oxidation behavior. A similar promotion of the soot oxidation behavior was found when combustion was carried out without gas phase oxygen, as reported in Figure 2 (dotted lines), which shows the weight loss of CZ/soot mixture against temperature in nitrogen atmosphere. In this case oxidation was driven exclusively by oxygen originating from ceria–zirconia and weight-loss accounted not only for the removal of carbon due to oxidation but also from oxygen loss from the lattice to give CO/CO_2.

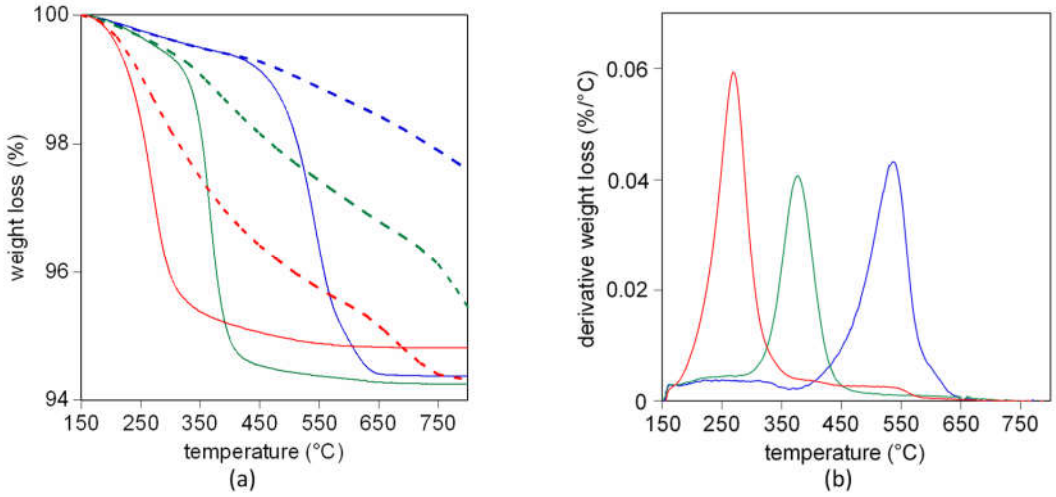

Figure 2. (**a**) Weight loss profile analysis of CZ/carbon mixtures in air (solid line) and in N_2 (dashed line) under different contact conditions and (**b**) derivative weight loss profile in air: CZ(l) (blue), CZ(t) (green) and CZ(m) (red).

Selectivity to CO_2 for each kind of contact could be obtained by a separate temperature programmed experiment carried out in N_2 atmosphere and monitoring CO/CO_2 evolution. As a first approximation CO_2 selectivity obtained can be used for estimating the amount of soot oxidized in TGA (Table 2). The results reported in Figure 2 and Table 2 indicate that the degree of contact strongly influenced oxidation also under inert atmosphere. In loose contact, due to the poorer distribution of soot over ceria, soot was oxidized more slowly (compare slope of the weight loss curves in Figure 2) and in smaller quantities. As the degree of contact increased, the exchange of the lattice oxygen of CZ with carbon was facilitated and much faster, leading to an overall calculated weight loss of 1.65% due to carbon and 3.95% due to oxygen for CZ(m). Although this value was lower than that observed under air (where complete carbon removal was observed with ca. 5.1% weight loss due to carbon), it indicates that transfer of oxygen from ceria to carbon played a key role in soot oxidation and was a strong function of the contact conditions.

Table 2. Summary of results for soot oxidation under inert conditions.

Sample	Total Weight Loss [a] (%)	Selectivity from TP Experiment [b] CO/CO_2	Calculated Weight Loss % (Carbon) [c]	Calculated Weight Loss % (Oxygen) [c]
CZ(l)	2.4	5/95	0.67	1.73
CZ(t)	4.6	10/90	1.32	3.28
CZ(m)	5.6	14/86	1.65	3.95

[a] total weight loss under inert atmosphere as measured from TGA experiment from 150 to 800 °C. [b] CO/CO_2 selectivity as measured in a temperature programmed oxidation experiment carried out from 150 to 800 °C under nitrogen atmosphere. [c] contribution of carbon and oxygen in total TGA weight loss calculated assuming selectivity measured in a TP experiment.

To further investigate the mechanism of oxygen transfer over different type of contact, the soot oxidation activity has been measured by running temperature programmed oxidation (TPO) experiments and using peak temperatures (Tp) as a measure of activity. As shown in Figure 3, by increasing the soot ceria contact, the oxidation temperature in O_2/N_2 significantly decreased (from 554 to 285 °C for loose and milled sample respectively), in agreement with T50 obtained from TGA.

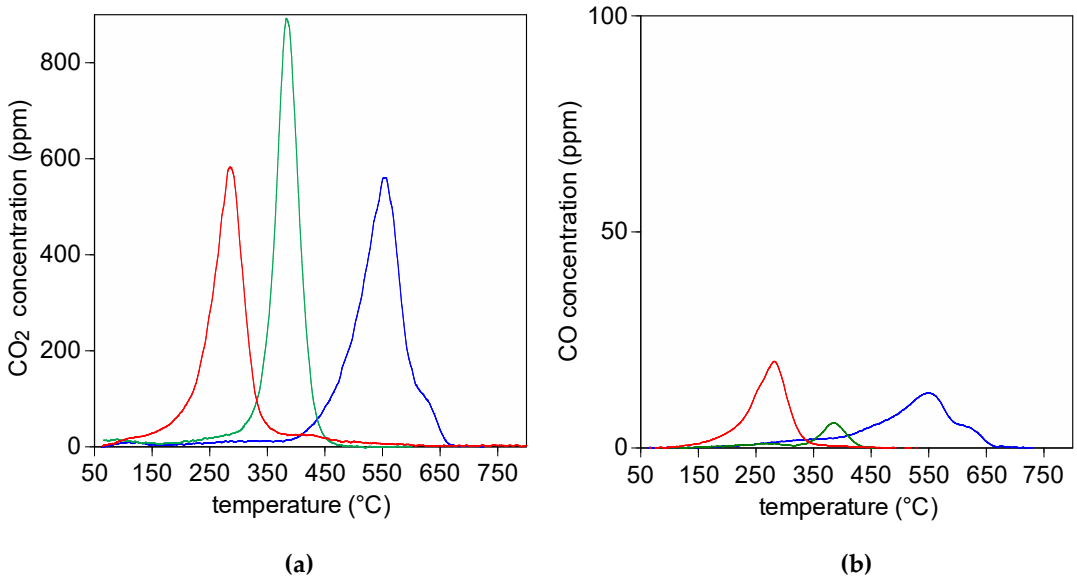

Figure 3. Temperature programmed oxidation (TPO) profiles of (**a**) CO_2 and (**b**) CO evolved from CZ/C mixtures at different mixing condition: CZ(l) (blue), CZ(t) (green) and CZ(m) (red).

Figure 3b shows the concentration of CO evolved during soot combustion. CO concentration was very low compared to CO_2, indicating higher selectivity for carbon dioxide, mainly due to the capability of ceria-zirconia catalyst to oxidize CO to CO_2 [17]. Contact conditions had a minor influence on the selectivity to CO_2, which changed from 99% under tight conditions to 97% for the loose and supertight contact mode.

The effect of the oxidation atmosphere (O_2/N_2, $NO/O_2/N_2$ and $NO_2/O_2/N_2$) in soot oxidation over the different catalyst/soot morphologies was investigated using TPO. The results are summarized in Table 3 and Figure 4. When the catalyst was in the loose contact mode, the use of a more oxidant mixture containing NO_x contributes to lower soot oxidation temperature by several degrees (from 554 to 515/516 °C) while, when CZ/soot was mixed in tight contact, less significant differences were found, in the range 378–383 °C. As expected, the presence of NO_x contributes to lower soot oxidation temperature by several degrees when the catalyst is in loose contact [18–20]. This is due to the oxidation of NO to NO_2 catalyzed by CZ and the subsequent carbon oxidation due to gas-phase NO_2, which is a more efficient oxidant than gas-phase O_2 [9]. With tight contact a very small positive contribution of NO_x atmosphere can be observed and the temperature of oxidation of carbon over NO_x/N_2 is only a few degrees lower compared to reaction in O_2/N_2 (378 vs. 383 °C). On the contrary, the presence of NO does not induce any promotion when more efficient contact is achieved using milled samples. The increased interfacial area between CZ and soot promotes active oxygen species formation at temperatures lower than that of the transformation of NO to NO_2 operated by ceria–zirconia. This does not allow formation of NO_2 before soot is already oxidized by oxygen, thus making ineffective the addition of NO. Looking at the details of peak temperatures, in the milled sample, the presence of NO_x in the gas phase slightly lowers the soot oxidation activity with a Tp increasing from 285 °C in O_2/N_2 to 294 °C in NO/N_2, indicating a general behavior in which soot oxidation for CZ(m) is favored under O_2/N_2. The creation of a thin layer of soot distributed on the catalyst with a high degree of contact at the nanoscale overcomes the limitation due to the poor mobility of active oxygen and boosts its oxidation potential.

Selectivity to CO_2 was always higher than 90% and slightly dependent on the composition of the gas stream (Table 3), with values close to 100% when only O_2 was present as an oxidant in the gas phase, independently on the type of contact. When NO_x species were added to the gas stream a lowering in CO_2 selectivity was observed, which is in agreement with data reported by García-García et al. [33,34]. Soot oxidation over ceria-based catalyst was connected with the formation of surface oxygenated species C(O) that act as intermediates in the formation of CO and CO_2 from thermal

decomposition and/or reaction of C(O) with "active oxygen" species [7,8,10,12,26,35]. When NO_x is present in the gas stream, two different reactions, NO adsorption and C(O) oxidation, compete over ceria active sites, both contributing to soot oxidation, but with NO adsorption competing with CO oxidation to CO_2 and consequently increasing CO production.

Table 3. Activity and selectivity results from TGA and TPO experiments.

		O_2/N_2 [a]		$NO/O_2/N_2$		$NO_2/O_2/N_2$	
sample	T50 (°C)	Tp (°C)	S_{CO2} (%)	Tp (°C)	S_{CO2} (%)	Tp (°C)	S_{CO2} (%)
CZ(l)	534	554	97	515	91	516	92
CZ(t)	364	383	99	378	95	377	96
CZ(m)	268	285	97	294	95	293	94

[a] TGA 21% O_2 in N_2; TPO 10% O_2 in N_2. 500 ppm NO/10% O_2 in N_2. 250 ppm NO_2/10% O_2 in N_2.

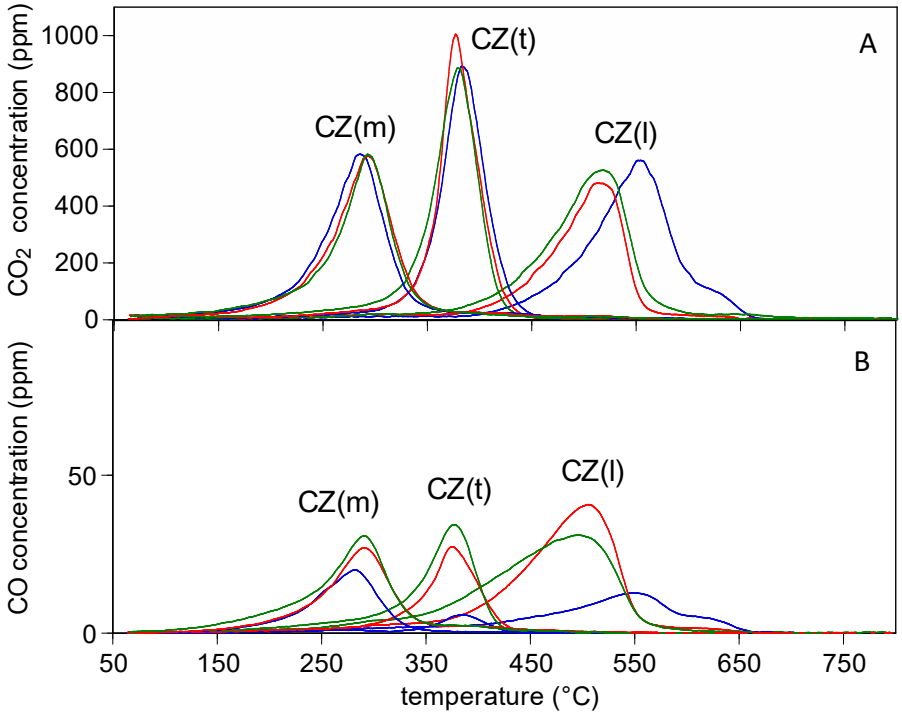

Figure 4. (**A**) CO_2 evolution and (**B**) CO evolution from temperature programmed oxidation (TPO) profiles for CZ/C mixtures at different mixing condition and different atmosphere: O_2 (blue), $NO+O_2$ (red) and NO_2+O_2 (green).

To further investigate the NO/NO_2 interaction with ceria–zirconia/soot mixtures, the NO oxidation profile over the $CeZrO_2$ oxide in the presence of soot was analyzed. Figure 5 shows the NO_2 concentration profile resulting from oxidation of NO. In general, formation of NO_2 started at a low temperature and was kinetically controlled. On increasing temperature (T > 500 °C) the opposite reaction predominated and the concentration of NO_2 decreased at values close to equilibrium. For samples in loose and tight contact, the onset of NO oxidation was at lower temperatures compared to milled samples (270 °C vs. 300 °C) indicating a higher NO oxidation rate and the overall NO_2 profile strongly differed from that observed in the CZ(m) sample. A decrease in NO_2 concentration (see circles in Figure 5) could be found in the range 490–560 °C and 340–390 °C, respectively for CZ(l) and CZ(t) mixtures. The decrease of NO conversion to NO_2 in these two samples was correlated to the decrease of oxygen concentration in these temperature ranges, as O_2 was consumed in carbon oxidation that peaks in the above temperature range, as indicated in Figure 5. This behavior was not observed in the case of CZ(m) because soot oxidation occurred at a temperature much lower to that of NO_2 production and NO_2 production occurred only after carbon was removed. This explains the

onset of NO oxidation at higher temperatures for CZ(m); the presence of a thin carbon shell around ceria–zirconia particles, hindered NO oxidation to NO_2, delaying NO_2 formation at higher temperatures, when the carbon envelope was completely oxidized by active oxygen species making accessible the ceria–zirconia catalyst surface to gas phase NO (Figure 6).

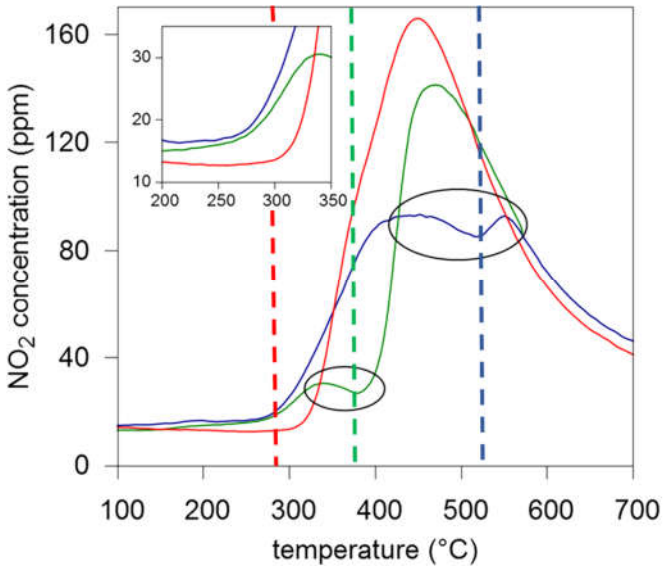

Figure 5. Temperature programmed oxidation (TPO) profiles of NO_2 evolved from CZ/C mixtures at different mixing condition under NO+O_2 gas flow: CZ(l) (blue), CZ(t) (green) and CZ(m) (red). Dotted lines indicate Tp of carbon oxidation (from red line in Figure 4).

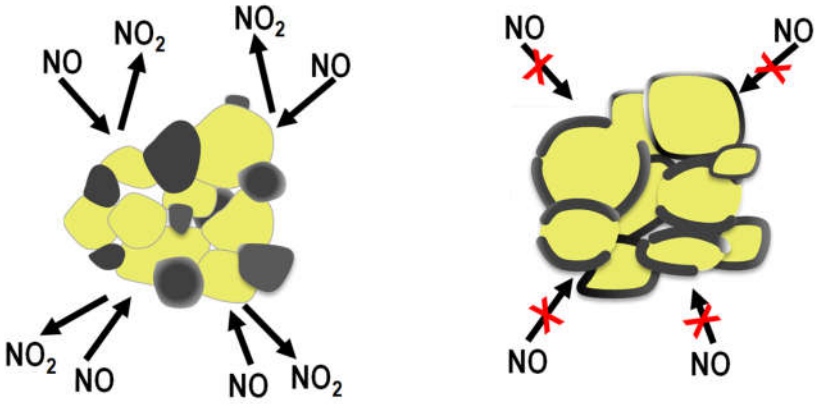

Figure 6. Scheme of NO_x interaction over CZ(t) and CZ(l) (left) and CZ(m) (right). Ceria–zirconia particles are indicated in yellow, while carbon agglomerates and carbon layers are indicated in black.

Summarizing, this study investigated the influence of nanoscale surface arrangements of the soot/catalyst mixture on the redox behavior of ceria–zirconia mixed oxide and on the reactivity of active surface oxygen species. The difference in the contact morphology between carbon soot and CZ particles strongly affected the oxygen transfer ability of ceria; in particular, increasing the carbon–ceria interfacial area, the reactivity of CZ lattice oxygen significantly improved. In addition, with a higher degree of contact, the soot oxidation was not affected by the presence of NO_x. Moreover, the existence of a core/shell structure strongly enhanced reactivity of interfacial oxygen species while affecting negatively NO oxidation characteristics.

3. Materials and Methods

Ceria–zirconia sample was prepared by coprecipitation of appropriate amount of ceria and zirconia precursors (cerium nitrate, $Ce(NO_3)_3{\cdot}6H_2O$ and zirconium nitrate, $Zr(NO_3)_2{\cdot}5H_2O$, Treibacher Industrie AG, Althofen, Austria) with NH_4OH in the presence of H_2O_2. The precipitate was dried overnight at 100 °C and calcined in air at 500 °C for 3 h. Ceria–zirconia composition in the solid solution was checked by XRD using the Rietveld refinement analysis (Table 1). Catalyst/soot mixtures were prepared by mixing a synthetic soot (Printex U by Degussa, Essen, Germany) with ceria–zirconia solid solution in a weight ratio 1:20. Printex U was selected as model soot due to its extensive use in literature; it is characterized by a C content of 96% and a surface area of 100 m^2/g. Loose contact was obtained by mixing the mixture in a vial for 2 min, while tight contact conditions were realized by grinding CZ and soot in an agate mortar for 10 min. Supertight contact was achieved milling ceria–zirconia particles and soot for 8 h in a high-energy Spex mill equipped with zirconia balls and a jar. Surface area measurements were carried out by means of a Tristar 3000 gas adsorption analyzer (Micromeritics, Norcross, GA, USA). X-ray diffraction patterns were recorded using a step size of 0.02° and a counting time of 40 s per angular abscissa in the range 20–145° on a Philips X'Pert diffractometer (40 kV and 40 mA, Ni-filtered Cu-Kα radiation, (PANalytical B.V., Almelo, The Netherlands). Phase identification was processed by Philips X'Pert HighScore software (Version 1.0b, PANalytical B.V., Almelo, The Netherlands), while mean crystalline size was estimated by the Scherrer [32] equation from the full width at the half maximum (FWHM) of the X-ray diffraction peak. The GSAS-EXPGUI program [36,37] was used for Rietveld refinement [38] of the XRD pattern

The carbon soot oxidation activity was followed by running temperature programmed oxidation (TPO) and thermogravimetric (TGA) experiments. In TPO the samples (ca. 20 mg) were treated by a fixed gas flow of 500 mL/min ($10\%O_2/N_2$, 500 ppm $NO_x/10\%O_2/N_2$ or 250 ppm $NO_2/10\%O_2/N_2$) from room temperature to 800 °C (heating rate 10 °C/min) with a GHSV ranging from 2.2 to $2.5 \times 10^6\ h^{-1}$. A chromel-alumel thermocouple was used to measure the temperature of the catalyst and the outlet composition was monitored by FT-IR gas analyzers (MultiGas 2030, MKS Instruments, Inc., Andover, MA, USA). Tp, peak-top temperature was used to compare the activity. Selectivity to CO_2 formation was determined by CO and CO_2 concentration in the outlet gas using the expression:

$$\text{Selectivity to } CO_2 = 100 \times C_{CO_2} / C_{CO_2} + C_{CO} \quad (1)$$

TGA experiments were carried out in a Q500, TA Instruments. The samples (ca. 20 mg) were first pretreated under inert atmosphere at 150 °C for 60 min to eliminate adsorbed water and then heated at a constant rate (10 °C/min) in air or N_2 (60 mL/min). T50, the temperature at which 50% of weight loss was obtained was used to compare the activity. Reproducibility in term of T50 and/or Tp in TPO and TGA experiments was always within ±5 °C and ±3 °C, respectively. Reproducibility tests on weight loss were carried out and have shown that the total weight loss for each type of contact was close to the nominal value with reproducibility within ±3% for CZ(m), and ±7% for CZ(t) and CZ(l).

4. Conclusions

In this study the effect of different atmosphere and contact conditions on soot combustion over a ceria-based catalyst was investigated to better understand the oxygen transfer ability and redox behavior of ceria–zirconia at low temperatures promoted by the use of carbon soot as a solid reductant. To accomplish this aim three different contact models were used with varying degrees of interfacial interaction between carbon and ceria–zirconia. The nanoscale carbon–ceria interface that we built using milling, although far from being representative of real conditions, can disclose information that are important in the understanding of oxidation properties of ceria. By increasing the numbers of contact points the temperature of soot oxidation in O_2 progressively decreased (from 550 to 280 °C). The effect of various oxidation atmospheres (O_2, $NO+O_2$ and NO_2+O_2) was investigated at different contact conditions. It appeared for example that oxygen atmosphere was best utilized for oxidation of carbon at the interface in close contact with ceria in contrast to the well-known properties of NO/O_2 mixtures that surpass oxygen when contact conditions are less robust. Therefore when the

interfacial ceria–zirconia/soot contact was strongly enhanced, gas phase O_2 promoted the formation of active oxygen through interfacial oxygen vacancies, resulting in a more powerful oxidant than NO_2. The presence of a ceria–zirconia core/carbon shell architecture strongly enhanced the reactivity of interfacial oxygen species while at the same time affecting negatively NO oxidation characteristics, by establishing a sort of protective shield, which did not allow ceria–zirconia to act as an oxidant for NO, thus preventing its action toward carbon. Therefore, the active oxygen species formed through interaction of the gas-phase oxygen with interfacial ceria vacancies immediately reacted with soot enhancing the combustion at very low temperature and hindering NO oxidation that usually takes place in that temperature range. This indicates that, even under an oxidizing atmosphere, the close and extended interfacial contact between ceria and carbon, allows the formation of oxygen vacancies, which then activate oxygen through the formation of well-known active oxygen species. This did not occur with the same intensity over CZ/carbon mixture prepared using the tight mode and did not occur at all over CZ(l), thus explaining the different level of activity toward oxygen and NO/NO_2. The above findings confirmed the key role of active oxygen species in soot oxidation with ceria-based materials and more importantly they disclosed the subtle but distinct redox chemistry of ceria with O_2 and NO/NO_2 mixtures at varying degree of interaction with carbon.

Author Contributions: Conceptualization, project administration, methodology, investigation, data curation, writing—original draft preparation, writing—review and editing, E.A.; Conceptualization, writing—original draft preparation, C.d.L.; Conceptualization, project administration, funding acquisition, methodology, resources, writing—review and editing, A.T. All authors have read and agreed to the published version of the manuscript.

Funding: This research was funded in part by Interreg V Italy-Austria project COAT4CATA project number ITAT1019.

Conflicts of Interest: The authors declare no conflict of interest.

References

1. Montini, T.; Melchionna, M.; Monai, M.; Fornasiero, P. Fundamentals and Catalytic Applications of CeO_2-Based Materials. *Chem. Rev.* **2016**, *116*, 5987–6041.
2. Aneggi, E.; Boaro, M.; Colussi, S.; de Leitenburg, C.; Trovarelli, A. Ceria-Based Materials in Catalysis: Historical Perspective and Future Trends. In *Handbook on the Physics and Chemistry of Rare Earths;* Elsevier: Amsterdam, The Netherlands, 2016; Volume 50, pp. 209–242.
3. Gorte, R.J. Ceria in Catalysis: From Automotive Applications to the Water Gas Shift Reaction. *AIChE J.* **2010**, *56*, 1126–1135.
4. Farrauto, R.J.; Heck, R.M. Catalytic converters: state of the art and perspectives. *Catal. Today* **1999**, *51*, 351–360.
5. Trovarelli, A. Catalytic properties of ceria and CeO_2-containing materials. *Catal. Rev.* **1996**, *38*, 439–520.
6. Di Monte, R.; Kaspar, J. On the role of oxygen storage in three-way catalysis. *Top Catal.* **2004**, *28*, 47–57.
7. Garcia, X.; Soler, L.; Divins, N.J.; Vendrell, X.; Serrano, I.; Lucentini, I.; Prat, J.; Solano, E.; Tallarida, M.; Escudero, C.; et al. Ceria-Based Catalysts Studied by Near Ambient Pressure X-ray Photoelectron Spectroscopy: A Review. *Catalysts* **2020**, *10*, 286.
8. Aneggi, E.; Leitenburg, C.D.; Trovarelli, A. Ceria-based formulations for catalysts for diesel soot combustion. In *Catalysis by Ceria and Related Materials*, 2nd Ed.; Alessandro, T., Paolo, F., eds.; Imperial College Press: London, UK, 2013.
9. Bueno-Lopez, A. Diesel soot combustion ceria catalysts. *Appl. Catal. B Environ.* **2014**, *146*, 1–11.
10. Krishna, K.; Bueno-Lopez, A.; Makkee, M.; Moulijn, J.A. Potential rare earth modified CeO_2 catalysts for soot oxidation I. Characterisation and catalytic activity with O_2. *Appl. Catal. B Environ.* **2007**, *75*, 189–200.
11. Konstandopoulos, A.G.; Pagkoura, C.; Lorentzou, S.; Kastrinaki, G. Catalytic Soot Oxidation: Effect of Ceria–Zirconia Catalyst Particle Size. *SAE Int. J. Engines* **2016**, *9*, 1709–1719.
12. Saab, E.; Abi-Aad, E.; Bokova, M.N.; Zhilinskaya, E.A.; Aboukais, A. EPR characterisation of carbon black in loose and tight contact with Al_2O_3 and CeO_2 catalysts. *Carbon* **2007**, *45*, 561–567.
13. Aneggi, E.; de Leitenburg, C.; Dolcetti, G.; Trovarelli, A. Promotional effect of rare earths and transition metals in the combustion of diesel soot over CeO_2 and CeO_2–ZrO_2. *Catal. Today* **2006**, *114*, 40–47.

14. Mukherjee, D.; Reddy, B.M. Noble metal-free CeO_2-based mixed oxides for CO and soot oxidation. *Catal. Today* **2018**, *309*, 227–235.
15. Simonsen, S.B.; Dahl, S.; Johnson, E.; Helveg, S. Ceria-catalyzed soot oxidation studied by environmental transmission electron microscopy. *J. Catal.* **2008**, *255*, 1–5.
16. Liu, S.; Wu, X.D.; Weng, D.; Ran, R. Ceria-based catalysts for soot oxidation: A review. *J. Rare Earth.* **2015**, *33*, 567–590.
17. Yang, Z.; Hu, W.; Zhang, N.; Li, Y.; Liao, Y. Facile synthesis of ceria–zirconia solid solutions with cubic–tetragonal interfaces and their enhanced catalytic performance in diesel soot oxidation. *J. Catal.* **2019**, *377*, 98–109.
18. Andana, T.; Piumetti, M.; Bensaid, S.; Russo, N.; Fino, D. Heterogeneous mechanism of NO_x-assisted soot oxidation in the passive regeneration of a bench-scale diesel particulate filter catalyzed with nanostructured equimolar ceria-praseodymia. *Appl. Catal. A Gen.* **2019**, *583*, 117136.
19. Andana, T.; Piumetti, M.; Bensaid, S.; Veyre, L.; Thieuleux, C.; Russo, N.; Fino, D.; Quadrelli, E.A.; Pirone, R. Nanostructured equimolar ceria-praseodymia for NO_x-assisted soot oxidation: Insight into Pr dominance over Pt nanoparticles and metal–support interaction. *Appl. Catal. B Environ.* **2018**, *226*, 147–161.
20. Matarrese, R.; Morandi, S.; Castoldi, L.; Villa, P.; Lietti, L. Removal of NO_x and soot over Ce/Zr/K/Me (Me = Fe, Pt, Ru, Au) oxide catalysts. *Appl. Catal. B Environ.* **2017**, *201*, 318–330.
21. Aneggi, E.; de Leitenburg, C.; Trovarelli, A. On the role of lattice/surface oxygen in ceria–zirconia catalysts for diesel soot combustion. *Catal. Today* **2012**, *181*, 108–115.
22. Bueno-Lopez, A.; Krishna, K.; Makkee, M.; Moulijn, J.A. Enhanced soot oxidation by lattice oxygen via La^{3+}-doped CeO_2. *J. Catal.* **2005**, *230*, 237–248.
23. Setiabudi, A.; Chen, J.L.; Mul, G.; Makkee, M.; Moulijn, J.A. CeO_2 catalysed soot oxidation—The role of active oxygen to accelerate the oxidation conversion. *Appl. Catal. B Environ.* **2004**, *51*, 9–19.
24. Bueno - Lopez, A.; Krishna, K.; Makkee, M.; Moulijn, J. Active oxygen from CeO_2 and its role in catalysed soot oxidation. *Catal. Lett.* **2005**, *99*, 203–205.
25. Zhu, L.; Yu, J.J.; Wang, X.Z. Oxidation treatment of diesel soot particulate on $Ce_xZr_{1-x}O_2$. *J. Hazard. Mater.* **2007**, *140*, 205–210.
26. Sartoretti, E.; Martini, F.; Piumetti, M.; Bensaid, S.; Russo, N.; Fino, D. Nanostructured Equimolar Ceria-Praseodymia for Total Oxidations in Low-O_2 Conditions. *Catalysts* **2020**, *10*, 165.
27. Machida, M.; Murata, Y.; Kishikawa, K.; Zhang, D.J.; Ikeue, K. On the reasons for high activity of CeO_2 catalyst for soot oxidation. *Chem. Mater.* **2008**, *20*, 4489–4494.
28. Aneggi, E.; Rico-Perez, V.; de Leitenburg, C.; Maschio, S.; Soler, L.; Llorca, J.; Trovarelli, A. Ceria-Zirconia Particles Wrapped in a 2D Carbon Envelope: Improved Low-Temperature Oxygen Transfer and Oxidation Activity. *Angew. Chem. Int. Edit.* **2015**, *54*, 14040–14043.
29. Aneggi, E.; Llorca, J.; Trovarelli, A.; Aouine, M.; Vernoux, P. In situ environmental HRTEM discloses low temperature carbon soot oxidation by ceria-zirconia at the nanoscale. *Chem. Commun.* **2019**, *55*, 3876–3878.
30. Soler, L.; Casanovas, A.; Escudero, C.; Perez-Dieste, V.; Aneggi, E.; Trovarelli, A.; Llorca, J. Ambient Pressure Photoemission Spectroscopy Reveals the Mechanism of Carbon Soot Oxidation in Ceria-Based Catalysts. *Chemcatchem* **2016**, *8*, 2748–2751.
31. Balaz, P.; Achimovicova, M.; Balaz, M.; Billik, P.; Cherkezova-Zheleva, Z.; Criado, J.M.; Delogu, F.; Dutkova, E.; Gaffet, E.; Gotor, F.J.; et al. Hallmarks of mechanochemistry: From nanoparticles to technology. *Chem. Soc. Rev.* **2013**, *42*, 7571–7637.
32. Jenkins, R.; Snyder, R.L. *Introduction to X-ray Powder Diffractometry*; Wiley: New York, NY, USA, 1996.
33. Giménez-Mañogil, J.; García-García, A. Opportunities for ceria-based mixed oxides versus commercial platinum-based catalysts in the soot combustion reaction. Mechanistic implications. *Fuel Process. Technol.* **2015**, *129*, 227–235.
34. Guillén-Hurtado, N.; López-Suárez, F.E.; Bueno-López, A.; García-García, A. Behavior of different soot combustion catalysts under NO_x/O_2. Importance of the catalyst–soot contact. *React. Kinet. Mech. Catal.* **2013**, *111*, 167–182
35. Zhang, W.; Niu, X.Y.; Chen, L.Q.; Yuan, F.L.; Zhu, Y.J. Soot Combustion over Nanostructured Ceria with Different Morphologies. *Sci. Rep. Uk* **2016**, *6*, 29062.
36. Larson, A.C.; Von Dreele, R.B. *General Structure Analysis System (GSAS)*; Los Alamos National Laboratory Report LAUR 86-748: Los Almos, NM, USA, **2000**.

37. Toby, B.H. EXPGUI, a graphical user interface for GSAS. *J. Appl. Crystallogr.* **2001**, *34*, 210–213.
38. Young, R.A. *The Rietveld Method;* IUCr Oxford University Press: New York, NY, USA, 1993.